Extended abstract
34th Conf. on Radar Meteorology
5-9 October 2009, Williamsburg, VA

P1.3 EVALUATION OF A MULTIPLE-DOPPLER VORTEX DETECTION AND CHARACTERIZATION TECHNIQUE USING REAL RADAR OBSERVATIONS

Corey K. Potvin*[,1], Alan Shapiro[1,2], and Jidong Gao[2]
[1]School of Meteorology, University of Oklahoma, Norman, OK
[2]Center for Analysis and Prediction of Storms, University of Oklahoma, Norman, OK

1. INTRODUCTION

During severe weather operations, forecasters often do not have time to thoroughly interrogate all incoming radar data. This is especially true when the forecast warning area exists within a multiple-Doppler domain. Objective detection algorithms become particularly important in such scenarios, serving to alert forecasters to important features they may otherwise have missed.

Since the implementation of the WSR-88D network, several algorithms have been developed to aid forecasters in real-time identification of intense tornado- and mesoscale vortices. These include the Tornado Vortex Signature (TVS) algorithm (Crum and Alberty 1993), the National Severe Storms Laboratory (NSSL) Mesocyclone Detection Algorithm (MDA; Stumpf et al. 1998) and the NSSL Tornado Detection Algorithm (TDA; Mitchell et al. 1998). Since these techniques rely upon gate-to-gate shear thresholds, they are particularly sensitive to noise in the velocity data.

The Velocity Track Display (VTD) technique and its variants (Lee et al. 1994; Roux and Marks 1996; Lee et al. 1999; Liou et al. 2006) fit radial velocity data to a vortex model in order to recover key characteristics of the vortex flow. This approach is less sensitive to noisy velocity data. Unfortunately, the VTD techniques are not designed to retrieve the vortex center, which instead must be predetermined using some other method. This makes the retrieval of the remaining vortex parameters particularly sensitive to errors in the specified vortex center when the vortex being retrieved is small relative to the observational resolution.

* Corresponding Author Address: Corey Potvin, 120 David L. Boren Blvd, Suite 5900, Norman, OK 73072; email: corey.potvin@ou.edu.

The method described herein also adopts a vortex-fitting approach. More specifically, radial wind observations from two or more close-proximity Doppler radars with overlapping domains are fit to an analytical low-order model of a vortex and near-environment. The multiple-Doppler nature of this technique makes it comparable to the dual-Doppler Extended Ground-Based VTD (EGBVTD; Liou et al. 2006). However, the model control parameters in our method include the vortex center, making *a priori* knowledge of the location of the vortex unnecessary. This allows the technique to function as a detection algorithm as well as a vortex characterization algorithm. The method is being designed for use in CASA (Collaborative Adaptive Sensing of the Atmosphere; McLaughlin et al. 2005; Brotzge et al. 2007) and CASA-like radar networks, whose high observational resolution and overlapping coverage permit more accurate detection and characterization of tornado- and mesocyclone-scale vortices when this approach is used.

A complete description of the original methodology as well as tests of the technique using analytically-generated, numerically-simulated and real tornadic wind fields were presented in Potvin et al. (2009). In the current study, recent improvements to the technique as well as new tests with real observations of tornado-like vortices are shown. The rest of the paper is organized as follows. The newest version of the low-order model is described in section 2. The retrieval methodology, including the computation and minimization of the cost function, is described in section 3. Section 4 describes the new detection criteria. Tests using WSR-88D observations of the 29 May 2004 Oklahoma tornadic supercell are presented in Section 5.

A summary and plans for future work follow in section 6.

2. LOW-ORDER MODEL

The low-order model to which the observed wind field is fit is comprised of four idealized flow fields: a uniform flow, linear shear flow and linear divergence flow (together comprising the "broadscale" flow), and a modified combined Rankine vortex (MCRV). An MCRV is actually a combination of two axisymmetric flow fields. The interior (or "core") of the MCRV is a solid body vortex. Outside of the MCRV core, the radial and tangential vortex winds decrease as a power of distance from the vortex center. The use of the MCRV model is supported qualitatively by high-resolution mobile radar observations of tornadoes (Wurman and Gill 2000; Bluestein et al. 2003; Lee and Wurman 2005). The vortex and the horizontal broadscale fields are allowed to translate, allowing radar data to be used at their actual locations and times of acquisition. A total of 19 parameters (Table 1) characterize the wind field in our low-order model. These parameters are considered constant over a single 4D retrieval domain. Thus, the low-order model will be violated in cases where the observed wind field rapidly evolves in time.

The broadscale portion of the model is described by

$$V_x = a + b(y - v_t t) + c\,(x - u_t t) + gz,$$
$$V_y = d + e(x - u_t t) + f\,(y - v_t t) + hz,$$

and the azimuthal velocity field v_θ and radial velocity field v_r of the MCRV are given by

$$v_\theta = \begin{cases} \dfrac{r}{R} V_T, & r < R, \\ \dfrac{R^\alpha}{r^\alpha} V_T, & r \geq R, \end{cases} \qquad v_r = \begin{cases} \dfrac{r}{R} V_R, & r < R, \\ \dfrac{R^\beta}{r^\beta} V_R, & r \geq R, \end{cases}$$

where

$$r = \sqrt{(x - x_0 - u_v t)^2 + (y - y_0 - v_v t)^2}$$

is the distance of a given (x, y) coordinate from the center of the vortex at time t. Casting the MCRV equations into Cartesian coordinates, adding the linear flow fields and taking the radial projection (with respect to a radar) of the result yields the model Doppler radar velocity, V_r^{mod}:

$$\begin{aligned} V_r^{mod} &= \cos\phi_n \sin\theta_n \left[a + b(y - v_b t) + c(x - u_b t) + gz + \frac{V_R}{R}(x - x_0 - u_v t) - \frac{V_T}{R}(y - y_0 - v_v t) \right] + \\ &\quad \cos\phi_n \cos\theta_n \left[d + e(x - u_b t) + f(y - v_b t) + hz + \frac{V_R}{R}(y - y_0 - v_v t) + \frac{V_T}{R}(x - x_0 - u_v t) \right] \\ &\quad r < R, \\ &= \cos\phi_n \sin\theta_n \left[a + b(y - v_b t) + c(x - u_b t) + gz + \frac{R^\beta V_R (x - x_0 - u_v t)}{r^{\beta+1}} - \frac{R^\alpha V_T (y - y_0 - v_v t)}{r^{\alpha+1}} \right] + \\ &\quad \cos\phi_n \cos\theta_n \left[d + e(x - u_b t) + f(y - v_b t) + hz + \frac{R^\beta V_R (y - y_0 - v_v t)}{r^{\beta+1}} + \frac{R^\alpha V_T (x - x_0 - u_v t)}{r^{\alpha+1}} \right] \\ &\quad r \geq R. \end{aligned} \tag{1}$$

where θ_n and ϕ_n are the azimuth and elevation angles, respectively, of the n^{th} radar (θ_n is measured clockwise from the north).

3. RETRIEVAL METHODOLOGY

Selection of Analysis Domains

The wind field retrievals are conducted within circular analysis domains that are sized according to the typical scales of the vortices we seek to detect. Using enough analysis domains to cover the entire dual-Doppler domain would, in the absence of a high performance computing cluster, require too much time for the technique to be applied in real-time. Therefore, retrievals are performed only in regions identified as possibly containing intense vortices. The process by which these regions are selected begins by identifying all pairs of azimuthally-adjacent radar gates (in both radar domains) that satisfy the following criteria: (1) the difference in radial velocity between the two radar gates exceeds 15 m s^{-1}; (2) the radial wind speed and reflectivity exceed 15 m s^{-1} and 20 dBZ (respectively) in at least one radar gate within 3 km of the gate pair centroid; (3) the radial wind speed exceeds 1 m s^{-1} in at least 75 % of all gates within 3 km of the gate pair centroid; and (4) < 20 % of the velocity data are missing within both 500 m and 1000 m of the gate pair centroid. Criteria 2 & 3 are intended to reduce the impact of spurious velocity data without increasing the risk of failing to identify regions containing intense vortices. Criterion 3 was found to be necessary in preliminary tests with observations collected by the CASA Integrated Project One (IP-1; Brotzge et al. 2007) radar testbed in Oklahoma due to the occasional occurrence of spurious velocity data in regions containing near-zero radial velocities. Criterion 4 was partly motivated by analytical experiments in which velocity data gaps produced spurious minima in J (not shown).

The centroid of each pair of radar gates satisfying the above criteria is stored. Since vortices always exhibit azimuthal shear signatures in the velocity fields of both radars (unlike linear shear zones), only centroids that are located within 2 km of another centroid in the other radar's domain are retained. All such points are then spatially grouped into clusters since there will generally be a multitude of such points associated with an intense vortex. Those clusters containing ten or more points have their centroids calculated and stored. Each of these centroids becomes the center of a grid of first guesses for the vortex center. Each first guess serves as the center of an analysis domain over which the wind field will be retrieved (Figure 1).

It is unknown whether these preliminary analysis domain selection criteria provide an optimal balance between the probability of detection, the false alarm rate, and computational time. However, they will be shown to be appropriate for the case examined herein. If future experiments reveal that a large number of analysis domains will inevitably be required in some cases, then parallel processing (e.g. using one processor per grid of analysis domains) could be used to produce acceptable computational wall clock times.

Cost function computation and minimization

Within each analysis domain, the (squared) discrepancies between the observed and model-predicted radial wind fields are summed over the spatial-temporal domains of N radars, each scanning in range r, azimuth θ and elevation angle ϕ. By taking the translation of the broadscale flow and vortex into account, discrepancy calculations for the radial wind model can be performed at the same locations and times as the observations. Since radar resolution volumes increase in size with distance from the radar, Doppler velocity observations become representative of winds over a larger region as range increases. A range-weighting factor, r_n^2/r^2_{mean}, is introduced to account for this.

The cost function J accounting for the discrepancies between the observed and model-predicted radial wind fields can therefore be represented by

$$J \equiv \sum_{n=1}^{N} \sum_{m=1}^{M} \sum_{\phi} \sum_{\theta} \sum_{r} \left(\frac{r_n}{r_{mean}} \right)^2 (V_r^{obs} - V_r^{mod})^2 \quad (2)$$

where M is the total number of full volume scans (temporal sum) and r_n is the radial distance of an observation point from the n^{th} radar (the range-weighting factor is appropriately modified in experiments with real data as described above). J provides a useful way to quantitatively compare the quality of retrievals for different experiments, and, when appropriately normalized, can be used to calculate the mean model error per radar grid point.

The cost function J is minimized to retrieve the set of parameter values producing the least squares error in the model wind (best fit between model and observed winds). In view of (2) and the location of the model parameters in (1), our minimization problem is highly non-linear. Conjugate gradient minimization methods have proven useful for such problems. The minimization algorithm used in this study is the Polak-Ribiere (1969) method, a robust and efficient variant of the Fletcher and Reeves (1964) algorithm. In both methods, the search direction is reset to that of steepest descent (with all previous direction and gradient information being discarded) every p iterations, where p is the number of model parameters.

As with other minimization techniques, multiple minima in J can prevent the desired minimum from being reached. Local minima in the current problem can result from the intrinsic non-linearity of the problem, as well as from areas of missing data and departures of the observed wind field from the model. In order to mitigate the problem of multiple minima, retrievals are performed for a multitude of first guess vortex centers. This increases the probability of detecting any tornadoes present within the analysis domain.

Unfortunately, the global minimum in J does not always correspond to the desired solution. This situation can occur when a tornado or other intense, small-scale vortex is embedded within a larger vortex or vortex-like circulation, such as a mesocyclone. In such cases, the larger circulation, by virtue of its larger "footprint", may fit the low-order model better than the smaller vortex, thus preventing the latter from being detected. In order to address this problem, the minimization procedure was initially split into two steps. In step 1, the vortex model parameters are fixed at zero (except for R since this would introduce a "division by zero" computational issue), and the broadscale parameters are retrieved. In step 2, the radial components of the wind field retrieved in step 1 are subtracted from the observed radial wind fields, and the retrieval is then repeated on the residual wind field. Since the flow retrieved in step 1 (and subtracted in step 2) is much more representative of the broadscale flow than of the tornadic flow, the tornadic component of the original flow dominates the residual field to be retrieved in step 2, thus improving the vortex retrieval and increasing the probability of detection.

Four-step retrieval procedure

The retrieval procedure has recently been expanded from two to four steps in order to allow the location and size of the analysis domain to be adjusted according to a preliminary vortex retrieval. This modification was motivated by the fact that, given any analysis domain size that is large enough to encompass most vortices of the type(s) being sought, the analysis domain will occasionally be much larger than the particular vortex being retrieved. In such cases, a smaller analysis domain would be desirable since it would allow the vortex to be more salient in the wind field to be retrieved.

The first two steps of the new procedure are the same as described above. At the end of step #2, if the retrieved $|V_T|$ exceeds a threshold value (10 m s^{-1} in this study), the retrieval proceeds to step #3; otherwise, the retrieval terminates and no vortex detection is made. Steps #3 and #4 are identical to steps #1 and #2 except the analysis domain is

modified according to the size and location of the vortex retrieved in step #2. The new analysis domain is centered on the retrieved vortex location valid midway through the period over which the retrieval is performed. The new analysis domain is resized such that the distance between its edge and the nearest point on the retrieved vortex core at the end of the retrieval period is 500 m. The analysis domain used in steps #3 and #4 is thus designed to be as small as possible while still encompassing the stronger vortex winds. If the modified analysis domain would be larger than the default domain, the modified analysis domain radius is set equal to the default domain radius.

If the V_T retrieved in step # 4 exceeds a threshold value, V_{det}, then a set of detection criteria (described in Section 4) is used to determine whether an intense vortex has been detected. Otherwise, no information is output and the retrieval procedure restarts at the next first guess vortex center.

Special treatment of vortex translation and position parameters

The vortex translation parameters are often the most difficult vortex parameters to retrieve. In cases where the distance traveled by the vortex during the retrieval period is small relative to the observational resolution, the intrinsic uncertainty in the vortex center creates a large flat region around the global minimum in $J(u_v, v_v)$. This is illustrated in Figure 2 for an analytically-generated vortex and background wind field. Flat regions in J tend to be problematic since they are more prone to containing local minima (common causes of which were listed above), thereby making the retrieved minimum more sensitive to the first guess.

Much more significant errors in the retrieved vortex translation parameters, as well as in the vortex location itself, can occur when multiple regions of azimuthal radial wind shear (including one or more vortices) exist within the analysis domain. In these cases, the retrieved vortex locations valid at the times of each radar scan may in reality correspond to two different features (two different vortices or one vortex and one shear zone). This can result in large errors in (u_v, v_v) and, if the feature "detected" in the first radar scan is not the vortex "detected" in the second radar scan, in (x_0, y_0) as well. The larger the errors in the first guess vortex location and translation velocity, the greater the probability of the technique mistakenly identifying two separate shear features as a single vortex.

In order to improve the retrieval of the vortex translation and location parameters, particularly in the situation just described, a series of steps is taken to obtain a better first guess for (u_v, v_v) and (x_0, y_0). First, before the wind retrieval is performed, the Gal-Chen (1982) advection retrieval method is applied to the reflectivity field within a circular domain (radius = 10 km) centered on the original analysis domain. Reflectivity data from the current and immediately previous scans of the nearest radar are used; the elevation angle is the same as that used in the wind retrieval. The retrieved reflectivity pattern translational velocity is then used as the first guess for the vortex translational velocity in step #2 of the retrieval procedure. At the end of step #2, J is calculated on a 4D grid of u_v, v_v, x_0 and y_0 values centered on the retrieved solution. The set of (u_v, v_v, x_0 and y_0) values with the smallest J is used as the first guess for these parameters in retrieval step #4. Ideally, this improved first guess will increase the probability that the minimization procedure converges to the desired solution.

4. DETECTION CRITERIA

One of the biggest challenges to developing appropriate detection criteria for this technique is the vortex parameter non-uniqueness problem described in Potvin et al. (2009). In cases where the actual vortex core is small relative to the observational resolution, the combination of the limited observational resolution and ellipticity (flatness) in J owing to the mathematical

nature of the vortex (MCRV) model can create numerous local minima. In particular, this problem frequently results in significant underestimation (overestimation) of R and overestimation (underestimation) of V_T. This is because, on the scale of the observational resolution, a strong, narrow (poorly-resolved) vortex resembles a weaker, wider (well-resolved) vortex and vice versa (Figure 3). It would therefore be dangerous to unconditionally use these parameters to distinguish between intense and weak vortices.

The approach we have adopted instead is to identify and utilize retrieved vortex characteristics that are verified by the velocity observations [this is a departure from the detection and characterization methodology used in Potvin et al. (2009)]. If the V_T retrieved in step #4 exceeds V_{det} (= 20 m s^{-1} in the tests below), then the outer (i.e. outside the vortex core) radius of n m s^{-1} tangential vortex wind, R_n, is calculated for the retrieved vortex for n = 10, 15, 20, and so on. The tangential (relative to the retrieved vortex center) components of the residual radial winds (calculated in retrieval step # 3 and treated as vectors here), V_{obs}', are also computed. For each value of n, all the V_{obs}' that exceed n and that are located within R_n of the vortex center are identified. If there exists at least one pair of such V_{obs}' that are separated from one another by > 90° relative to the vortex center, then the values of n and R_n are output to the user (this minimum angular separation criterion helps prevent regions of strong linear shear from being identified as strong vortices). If the maximum n meeting these criteria, V_T^{res}, exceeds V_{det}, then the vortex is tentatively classified a detection. This approach is inherently conservative since the radial (residual) winds from which the V_{obs}' are calculated are themselves only components of the total velocities, meaning that the V_{obs}' and thus V_T^{res} will generally be underestimates.

Preliminary detections are subsequently subjected to a set of criteria designed to filter spurious retrievals. If ≥ 25 % of the velocity data located within R_n of the retrieved vortex center are missing, or if the portion of the retrieved vortex with $V_\theta > n$ extends outside of the analysis domain, the retrieval is rejected since data edges often give rise to local minima. The retrieval is also rejected if the root-mean-square (rms) error (difference between observed and retrieved radial velocity) computed within R_n of the retrieved vortex exceeds the rms observed velocity over that same area. This criterion is crucial since retrievals that provide a poor match to the observed wind field can nevertheless be associated with local minima in the typically highly complex cost function surface.

5. EXPERIMENTS WITH SMART RADAR OBSERVATIONS OF 29 MAY 2004 SUPERCELL

Case Overview

A supercell that spawned a series of tornadoes across Oklahoma during the evening of 29 May 2004 was observed by both a Doppler On Wheels radar (DOW; Wurman et al. 1997) and a pair of Shared Mobile Atmospheric Research and Teaching (SMART; Biggerstaff et al. 2005) radars near Geary and Calumet, OK. Selected images of reflectivity and radial velocity from the DOW dataset can be viewed at http://www.cswr.org/dataimages/rotate/geary-summary-2004-0711fp.pdf. De-aliased and quality-controlled data collected by the SMART radars were used to test our technique. More specifically, the base elevation (0.5°) scans from four consecutive volume scans beginning at 0022 Z, 0027 Z, 0033 Z and 0038 Z were used. The range and azimuthal sampling intervals for both radars were approximately 67 m and 1°, respectively. The distance between each of the radars and the analysis domains varied between ~20 km and ~50 km in these tests, yielding azimuthal sampling intervals of between ~350 m and ~850 m. Each analysis domain grid consisted of nine first guess

vortex centers separated by 500 m in the x- and y-directions. The initial analysis domain radius was set to 2 km.

The supercell examined here was unusual in that it contained a very strong 1-2 km diameter vortex that extended to the surface. Several smaller vortices (≤ 1 km core diameter) formed and died within the larger circulation during the SMART radar observing period. These vortices are indicated in the individual radars' data by regions of enhanced shear. However, the strongest measured winds occurred outside of these vortices, within the parent circulation. Since the smaller-scale vortices are not readily visually discernable from the surrounding mesoscale vortex flow, this is a useful test case for our algorithm. The existence of these smaller vortices is confirmed by the presence of intense shear and reflectivity holes (or "eyes") in the higher-resolution DOW data. Which of these vortices actually extended to the surface as tornadoes, and whether or not the mesoscale vortex itself ought to be labeled a tornado, is not important in these experiments. Our goal here is to verify that the technique is capable of detecting and characterizing intense small-scale vortices.

Results

The criteria used to identify regions of the radar domain within which to perform wind retrievals (Section 3) worked well at all four analysis times. All of the small-scale vortices evident within the mesoscale circulation were contained within one or more of the identified regions, and the numbers of identified regions were not prohibitively high, varying between 4 and 12 per analysis time. In all cases where a detection occurred, the existence of an intense vortex was supported by both the similarity of the retrieved vortex wind field to the residual (observed minus retrieved broadscale) wind field, and the resemblance of the total retrieved wind field to the observed radial velocity fields. Plots of the DOW velocity and reflectivity data further corroborated the existence of these vortices.

Since forecasters must analyze large amounts of information during severe weather operations, it may be prudent to have the algorithm output a single set of vortex characteristic estimates from each set of detections likely corresponding to the same vortex (e.g. located within 500 m of one another), rather than estimates from each individual retrieval. Thus, the ensemble (calculated over all retrievals passing the detection criteria) means of the most important retrieved vortex characteristics were computed at each analysis time in these tests (Table 2). In order to evaluate how well the mean retrieved vortex characteristics represent the actual vortex in each case, the radial component of the retrieval most closely approximating the ensemble mean retrieval for each analysis time was plotted and compared to the observed radial velocity field (Figures 4-7). In all four cases, the broadscale portion of the model, though linear, recovered the larger scale (parent vortex) circulation sufficiently well that the embedded vortices were salient in the residual flow. The vortex itself was subsequently accurately retrieved (at least on observed scales).

Though the "true" values of R_{20}, V_T, etc. cannot be precisely determined (and will not even be well-defined in some cases, e.g. elliptical vortices), the retrieved values of these parameters can be qualitatively evaluated through comparison of the retrieved and observed wind fields. In all four cases, the observed and retrieved total radial velocity fields are reasonably similar to one another, as are the residual and retrieved vortex radial velocity fields. The mean R_{20} is largest for the 0033 Z analysis, which appears to contain the largest vortex out of the four analysis times. In addition, the fact that the observed radial velocities in this vortex are stronger than in the other vortices is represented in the higher mean value of V_{Tres} (33 m s^{-1}) in this case. It is also encouraging that the retrievals capture the strong convergence indicated in the radial wind observation fields at 0022 Z (most evident at x = 2.25 km, y = 19 km in Figure

4b) and 0033 Z (most evident at x = -33 km, y = 23.5 km in Figure 7a).

The standard deviations in the retrieved vortex characteristics were also calculated to provide a proxy for the uncertainty in these estimates (Table 3). These indicate that while the uncertainty in the retrieved vortex center is small at each analysis time, the uncertainty in the vortex translational velocity can be significant. This is partly because the vortices do not move very far relative to the uncertainty in their initial and final positions (see Section 3). Using longer inter-scan intervals likely would not improve the (u_v, v_v) retrieval in this case given the long return period between scans (~5 min) and the fact that vortices were continually forming and dissipating in close proximity to each other. However, the higher temporal resolution afforded by a CASA-like radar system would make this approach to improving (u_v, v_v) more feasible. Table 3 also shows that the uncertainty tends to be significantly larger in the vortex model parameters (V_T, α *and* R) than in the quantities derived from them (e.g. R_{20} and V_{Tres}). Thus, our solution to the vortex solution non-uniqueness problem (see Section 4) appears to work well in these tests.

6. SUMMARY AND FUTURE WORK

A new multiple-Doppler vortex detection and characterization technique is being developed and tested. The technique utilizes the dense, overlapping Doppler velocity coverage provided by CASA-like radar networks to retrieve important vortex characteristics such as location, size and strength. These characteristics are determined by least-squares fitting the radial wind observations to a low-order model of a vortex and surrounding flow.

Several recent improvements to the technique are discussed in this paper. The retrieval procedure has been extended to allow the analysis domain to be relocated and resized based on a preliminary vortex retrieval. This helps ensure that the analysis domain is as small as possible (thereby making the vortex more dominant in the wind field to be retrieved) while still encompassing the stronger vortex winds. The use of this extended retrieval procedure has also permitted the implementation of a scheme for improving the first guess and therefore improving the retrieved values of the vortex location and translational velocity parameters, especially in cases where the vortex displacement between consecutive radar scans is large. Finally, the detection criteria have been redesigned to determine whether retrieved vortex characteristics are consistent with the observed wind field before being considered trustworthy. Such a "reality check" is critical because of the existence of multiple minima in the cost function, especially those associated with non-uniqueness in the MCRV model parameters.

Experiments with real dual-Doppler observations of several intense vortices that occurred within the 29 May 2004 Oklahoma supercell indicate the technique is capable of detecting and characterizing vortices reasonably well, even when they are embedded within a larger and stronger vortex. These results indicate the technique should be beneficial to tornado warning operations, especially during fast-paced severe weather operations or when multiple scales of rotation are present within a storm.

The technique will be tested with additional multiple-Doppler observations of intense vortices. The ability of the technique to characterize vortices > 1 km in diameter using both single- and dual-Doppler observations will also be explored. Special emphasis will be placed on the technique's potential to anticipate tornadogenesis through detection and characterization of incipient tornadoes and low-level mesocyclones.

Acknowledgements: The work presented herein was primarily supported by NSF grant EEC-031347, through the Engineering Research Center (ERC) for Collaborative Adaptive Sensing of the Atmosphere (CASA). The SMART radar data were collected and provided by Dr. M. Biggerstaff and edited by

K. Kuhlman and D. Betten under NSF grant ATM-0802717.

REFERENCES

Biggerstaff, M.I., L.J. Wicker, J. Guynes, C. Ziegler, J.M. Straka, E.N. Rasmussen, A. Doggett, L.D. Carey, J.L. Schroeder, and C. Weiss, 2005: The Shared Mobile Atmospheric Research and Teaching Radar: A Collaboration to Enhance Research and Teaching. *Bull. Amer. Meteor. Soc.*, **86**, 1263–1274.

Bluestein, H. B., W.-C. Lee, M. Bell, C. C. Weiss, and A. L. Pazmany, 2003: Mobile Doppler radar observations of a tornado in a supercell near Bassett, Nebraska, on 5 June 1999. Part II: Tornado-vortex structure. *Mon. Wea. Rev*., **131**, 2968–2984.

Brotzge, J., K. Brewster, V. Chandrasekar, B. Philips, S. Hill, K. Hondl, B. Johnson, E. Lyons, D. McLaughlin, and D. Westbrook, 2007: CASA IP1: Network operations and initial data. Preprints, *87th AMS Annual Meeting*, San Antonio, TX, Amer. Meteor. Soc.

Center for Severe Weather Research, cited 2009: Preliminary Radar Analysis of the Geary-Calumet, Oklahoma Tornadoes Occurring on 29 May 2004. [Available online at http://www.ametsoc.org/pubs/ journals/author_reference_guide.pdf.]

Crum, T. D., and R. L. Alberty, 1993: The WSR-88D and the WSR-88D Operational Support Facility. *Bull. Amer. Meteor. Soc*., **74**, 1669–1687.

Fletcher, R., and C.M. Reeves, 1964: Function minimization by conjugate-gradients. *Computer J.,* **7**, 149-153.

Gal-Chen, T., 1982: Errors in Fixed and Moving Frames of Reference: Applications for Conventional and Doppler Radar Analysis. *J. Atmos. Sci.*, **39**, 2279–2300.

Lee, W.-C., and J. Wurman, 2005: Diagnosed three-dimensional axisymmetric structure of the Mulhall tornado on 3 May 1999. *J. Atmos. Sci*., **62**, 2373-2393.

——, F. D. Marks, Jr., and R. E. Carbone, 1994: Velocity Track Display – A technique to extract real-time tropical cyclone circulations using a single airborne Doppler radar. *J. Atmos. Oceanic Technol*., **11**, 337–356.

——, J.-D. Jou, P.-L. Chang, and S.-M. Deng, 1999: Tropical cyclone kinematic structure retrieved from single Doppler radar observations. Part I: Interpretation of Doppler velocity patterns and the GBVTD technique. *Mon. Wea. Rev.*, **127**, 2419-2439.

Liou, Y.-C., T.-C. Chen Wang, W.-C. Lee, and Y.-J. Chang, 2006: The retrieval of asymmetric tropical cyclone structures using Doppler radar simulations and observations with the Extended GBVTD technique. *Mon. Wea. Rev*., **134**, 1140-1160.

McLaughlin, D., V. Chandrasekar, K. Droegemeier, S. Frasier, J. Kurose, F. Junyent, B. Philips, S. Cruz-Pol, and J. Colom, 2005: Distributed Collaborative Adaptive Sensing (DCAS) for improved detection, understanding, and predicting of atmospheric hazards. Preprints*, 85th AMS Annual Meeting,* San Diego, CA, Amer. Meteor. Soc.

Mitchell, E. D., 1995: An enhanced NSSL tornado detection algorithm. Preprints, *27th Conf. on Radar Meteorology*, Vail, CO, Amer. Meteor. Soc., 406–408.

Polak, E. And G. Ribiere, 1969: Note sur la convergence de methods de directions conjuguees. Rev. Franc. Informat. Rech. Operationnelle, **16**, 35-43.

Potvin, C.K., A. Shapiro, T.Y. Yu, J. Gao, and M. Xue, 2009: Using a Low-Order Model to Detect and Characterize Tornadoes in Multiple-Doppler Radar Data. *Mon. Wea. Rev.*, **137**, 1230–1249.

Roux, F., and F. D. Marks, 1996: Extended velocity track display (EVTD): An improved processing method for Doppler radar observation of tropical cyclones. *J. Atmos. Oceanic Technol.*, **13**, 875–899.

Smith, T. M., and K. L. Elmore, 2004: The use of radial velocity derivatives to diagnose

rotation and divergence. Preprints, *11th Conf. on Aviation, Range and Aerospace*, Hyannis, MA, Amer. Meteor. Soc.

Stumpf, J. G., Witt, A., Mitchell, E. D., Spencer, P. L., Johnson, J. T., Eilts, M. D., Thomas, K. W., and D. W. Burgess, 1998: The National Severe Storms Laboratory Mesocyclone Detection Algorithm for the WSR-88D. *Wea. Forecasting*, **13**, 304-326.

Wurman, J., and S. Gill, 2000: Finescale radar observations of the Dimmitt, Texas (2 June 1995), tornado. *Mon. Wea. Rev.*, **128**, 2135-2164.

——, J. Straka, E. Rasmussen, M. Randall, and A. Zahrai, 1997: Design and deployment of a portable, pencil-beam, pulsed, 3-cm Doppler radar. *J. Atmos. Oceanic Technol.*, **14**, 1502-1512.

Table 1. Description of low-order model parameters.

Parameter	Description
a ($m\ s^{-1}$)	Uniform flow velocity
d ($m\ s^{-1}$)	
b (s^{-1})	Horizontal shear amplitudes
e (s^{-1})	
c (s^{-1})	Horizontal divergence amplitudes
f (s^{-1})	
g (s^{-1})	Vertical shear amplitudes
h (s^{-1})	
R (m)	Vortex radius of maximum wind
V_R ($m\ s^{-1}$)	Maximum radial, tangential winds
V_T ($m\ s^{-1}$)	
x_0 (m)	Vortex center location
y_0 (m)	
u_b ($m\ s^{-1}$)	Broadscale translational velocity
v_b ($m\ s^{-1}$)	
u_v ($m\ s^{-1}$)	Vortex translational velocity
v_v ($m\ s^{-1}$)	
α	Vortex wind decay
β	

Table 2. Means of retrieved vortex characteristics for each set of retrievals.

Time	Distance from ensemble mean vortex center (m)	Movement ($m\ s^{-1}$)	Heading (°clockwise from east)	V_T ($m\ s^{-1}$)	V_T^{res} ($m\ s^{-1}$)	V_R ($m\ s^{-1}$)	R (m)	R_{20} (m)	R_{25} (m)	R_{30} (m)	R_{35} (m)
0022Z	78	29	-33	28	21	-20	393	555	*N/A*	*N/A*	*N/A*
0027Z	81	9	-46	40	20	1	223	519	*N/A*	*N/A*	*N/A*
0033Z	80	15	28	62	33	-13	369	845	713	622	551
0038Z	133	11	-70	50	20	1	332	684	*N/A*	*N/A*	*N/A*

Table 3. Standard deviations of retrieved vortex characteristics for each set of retrievals. Asterisked values indicate standard deviations that have been recomputed upon removing an extreme outlier.

Time	Distance from ensemble mean vortex center (m)	Movement ($m\ s^{-1}$)	Heading (°clockwise from east)	V_T ($m\ s^{-1}$)	V_T^{res} ($m\ s^{-1}$)	V_R ($m\ s^{-1}$)	R (m)	R_{20} (m)	R_{25} (m)	R_{30} (m)	R_{35} (m)
0022Z	57	5	3	3	3	3	166	133	*N/A*	*N/A*	*N/A*
0027Z	101 (55*)	6	26	6	0	2	44	88	*N/A*	*N/A*	*N/A*
0033Z	55	6	40 (19*)	7	2	6	69	72	76	80	91
0038Z	81	4	27	4	0	1	174	139	*N/A*	*N/A*	*N/A*

Figure 1. Schematic illustrating the procedure for selecting the wind retrieval domains.

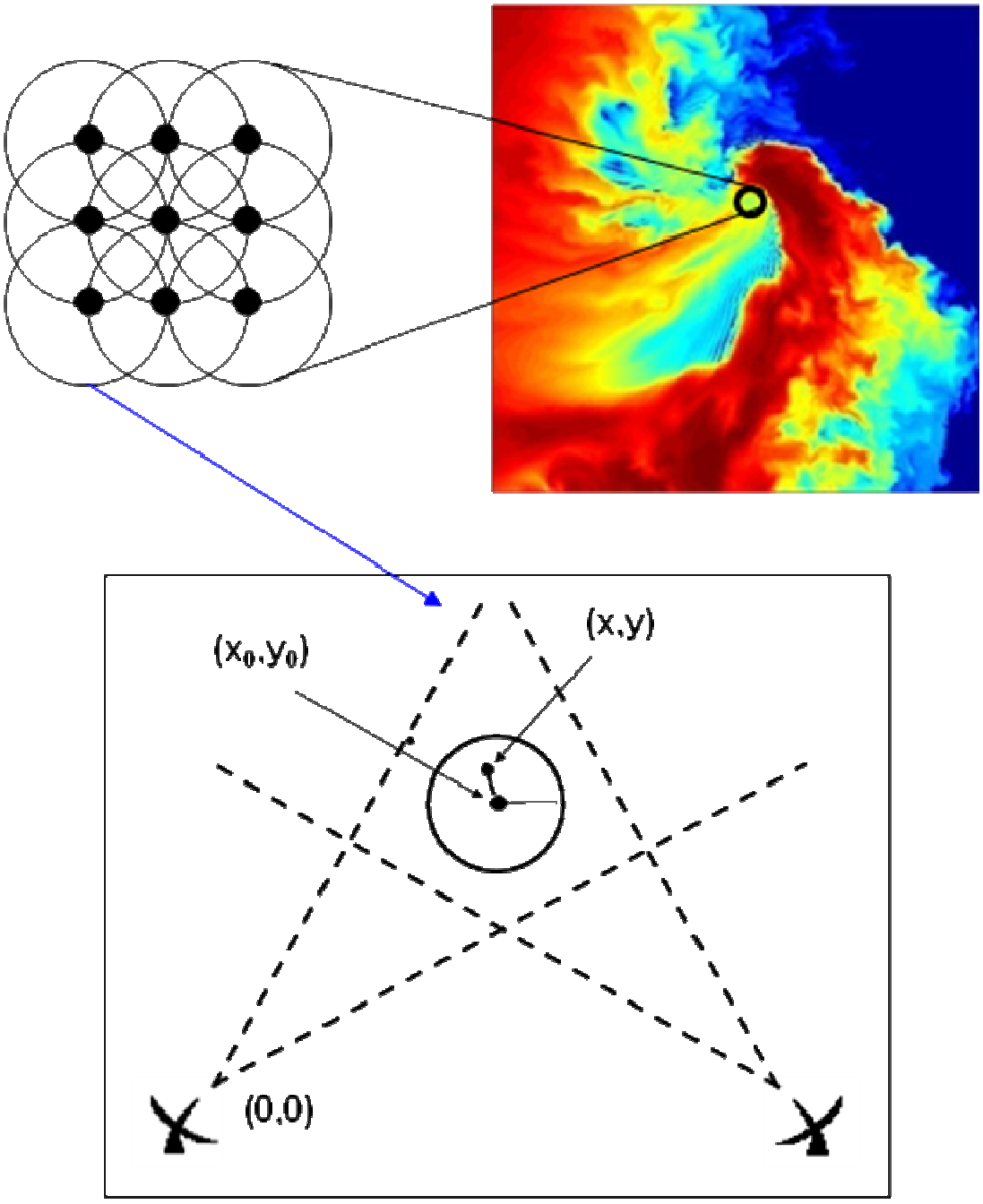

Figure 2. $J(u_v, v_v)$ (10^6 m^2 s^{-2}) for an analytical vortex with true (u_v, v_v) = 10 m s^{-1}. Remaining parameters are set to their true values.

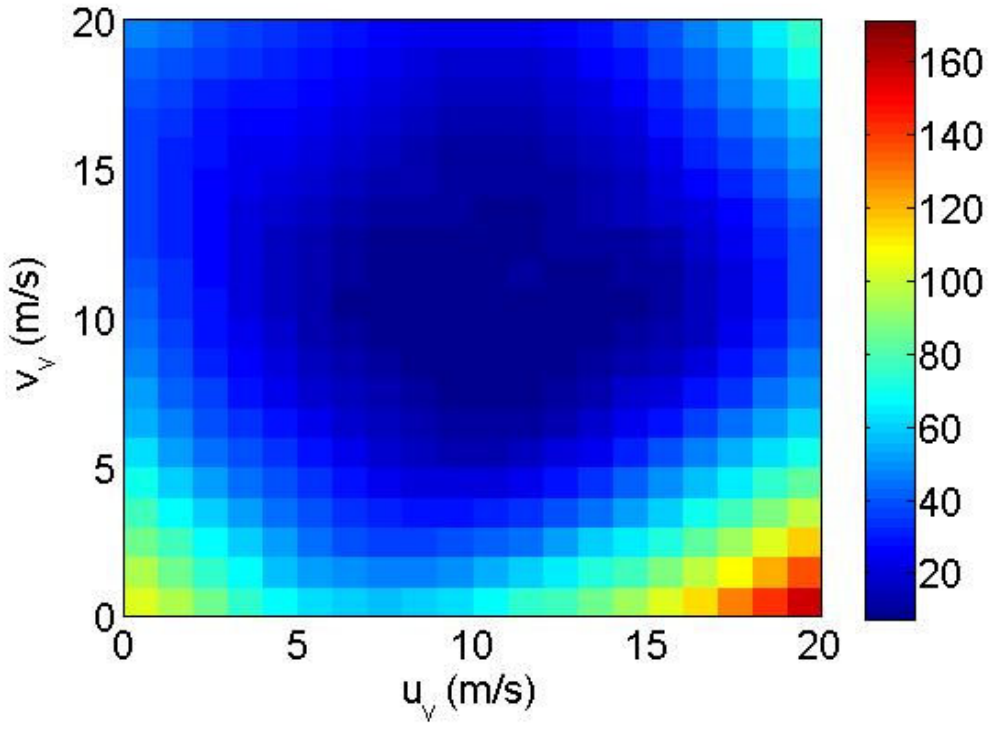

Figure 3. Tangential velocity profiles for two very different MCRVs. The black dots represent the centers of hypothetical radar probe volumes separated by 200 m.

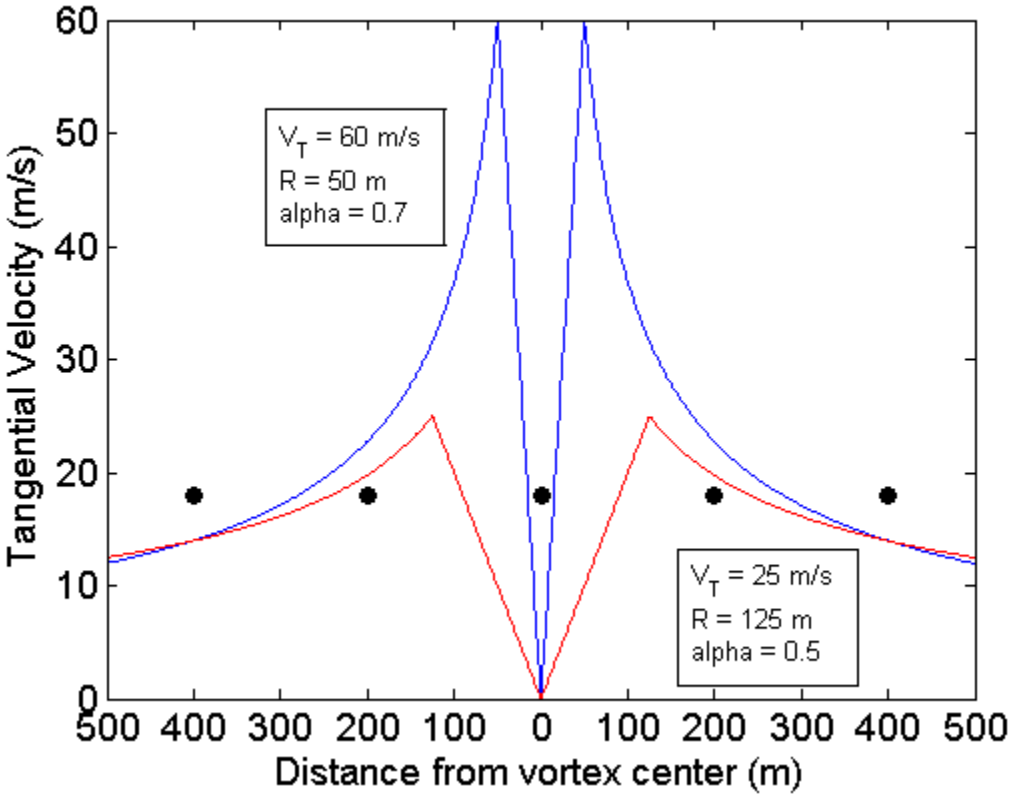

Figure 4. Clockwise from top left: observed, residual (observed minus retrieved broadscale), retrieved vortex, and retrieved total radial velocity fields at 0022 Z for radars located (a) southeast and (b) southwest of the analysis domain. The axes indicate *x*- and *y*-displacements from the radar.

(a)

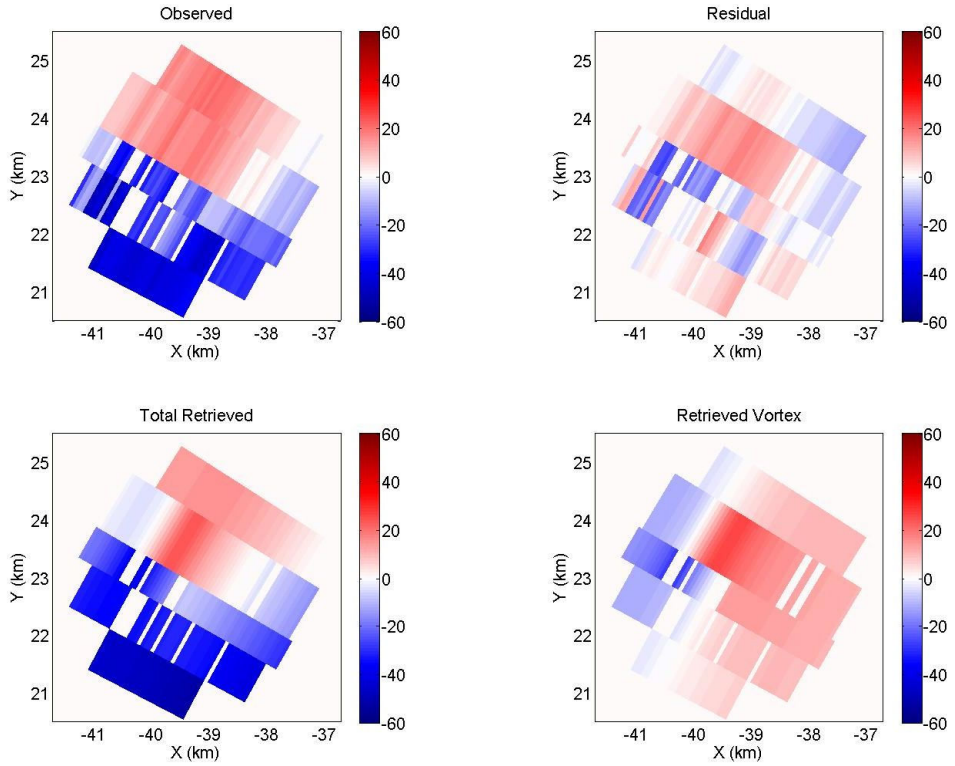

(b)

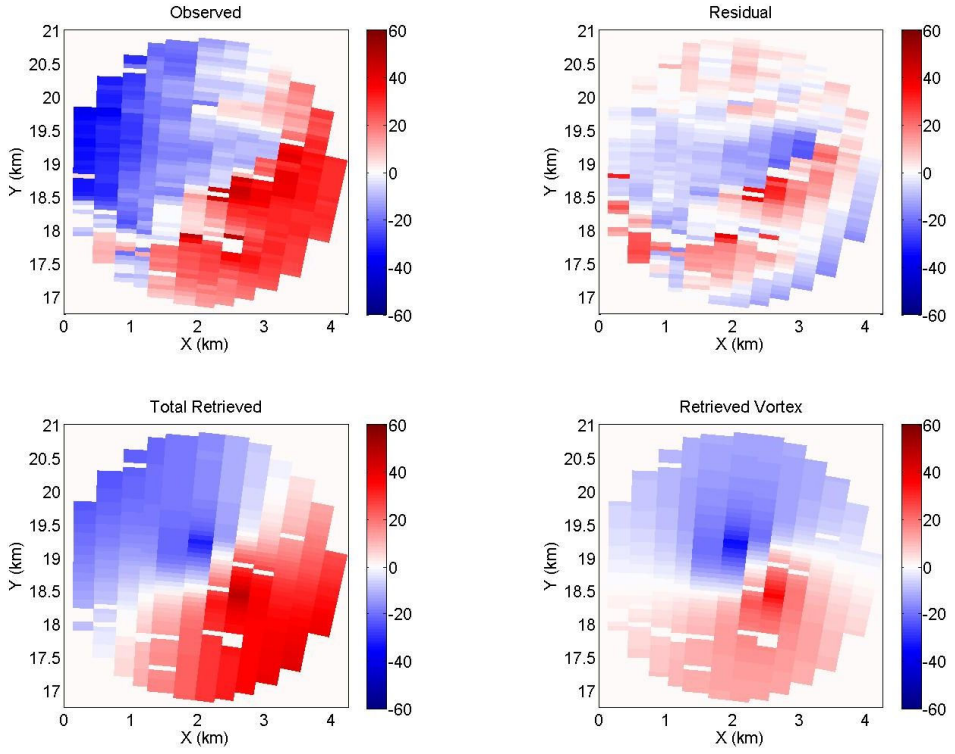

Figure 5. Same as Fig. 4 except at 0027 Z.

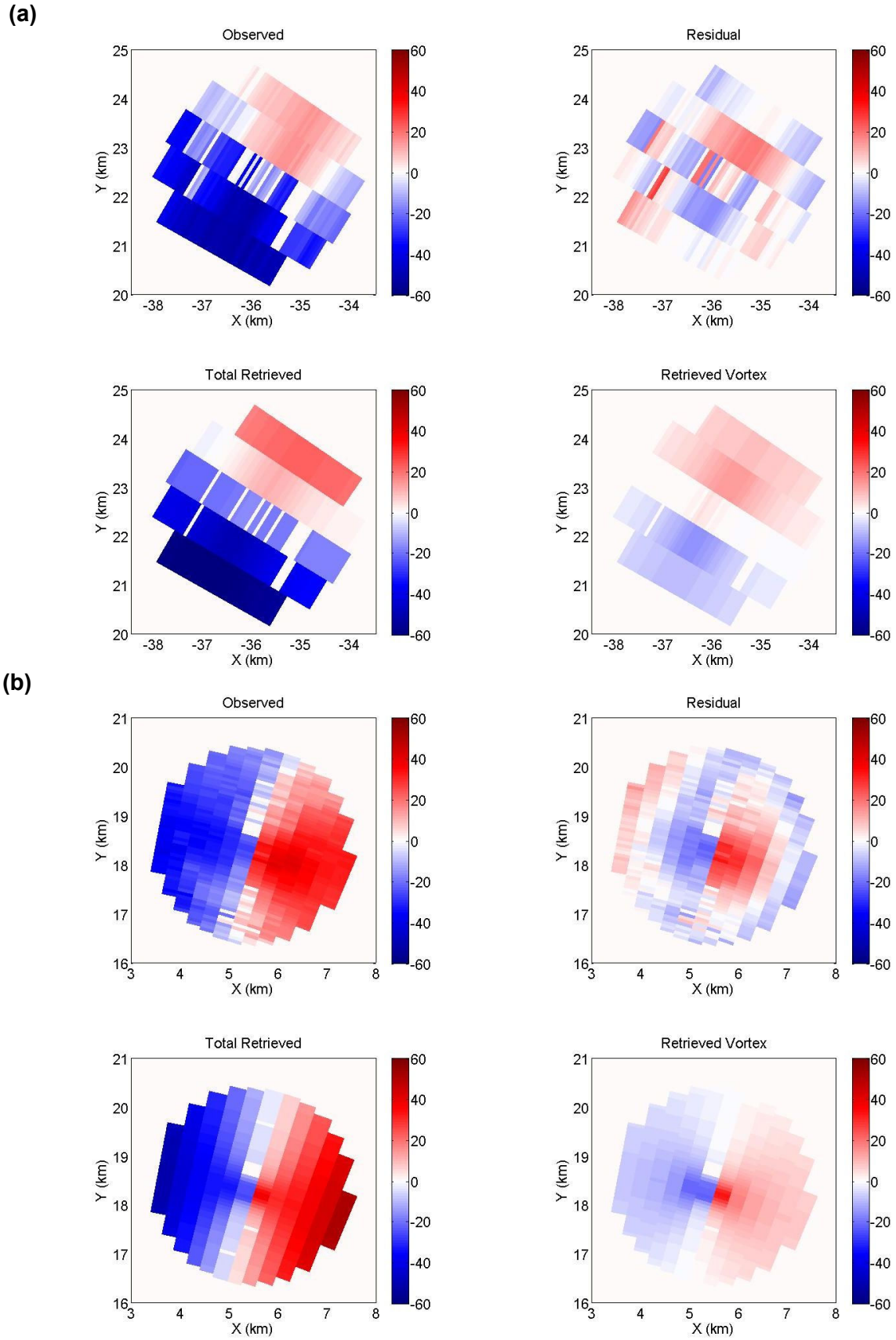

Figure 6. Same as Fig. 4 except at 0033 Z.

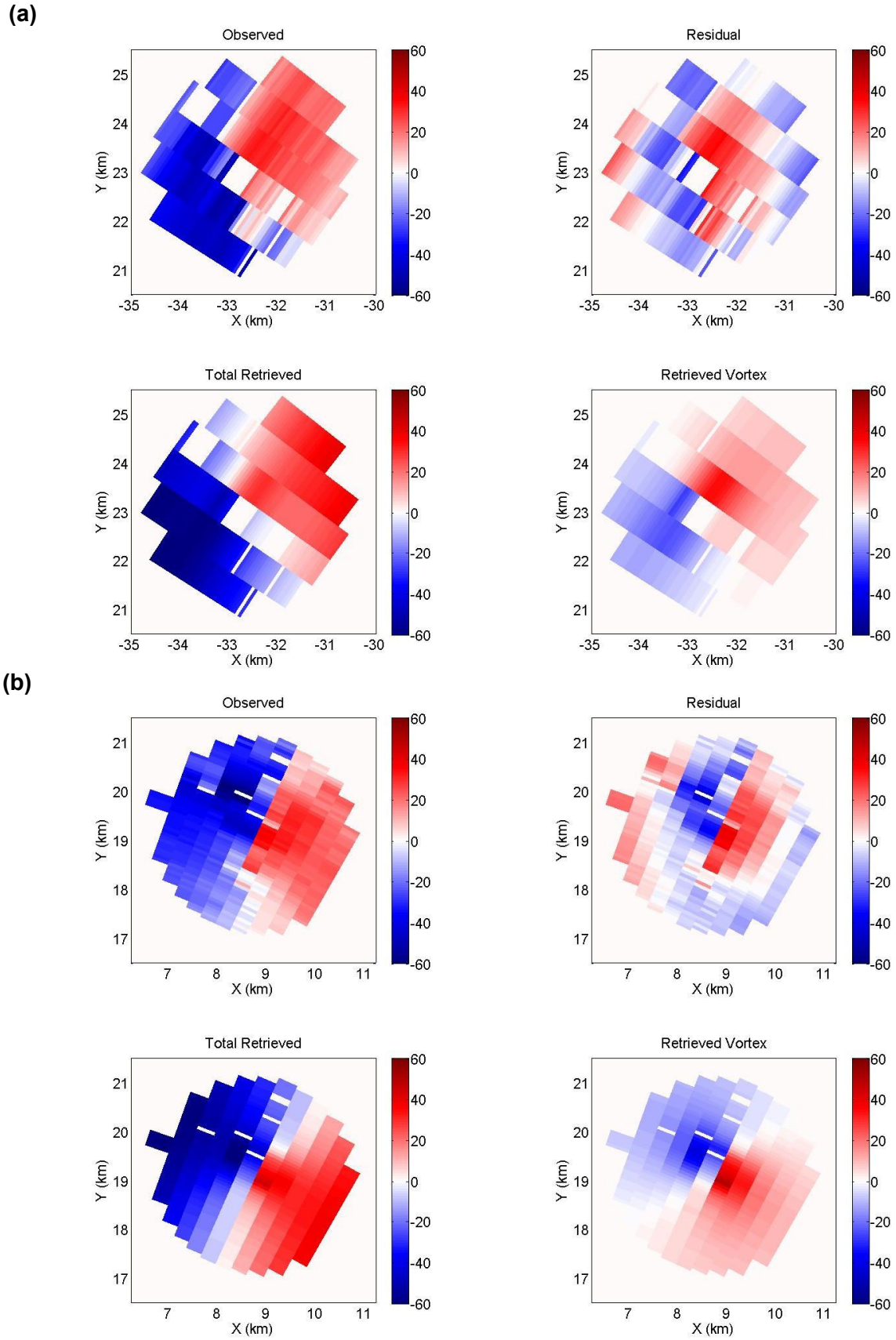

Figure 7. Same as Fig. 4 except at 0038 Z.